2011 American Control Conference
on O'Farrell Street, San Francisco, CA, USA
June 29 - July 01, 2011

Li-ion Battery Parameter Estimation for State of Charge

Xidong Tang, Xiaofeng Mao, Jian Lin, and Brian Koch

Abstract—**Battery state of charge (SOC) is a critical parameter for the control of propulsion systems in plug-in hybrid electric vehicles (PHEV) and electric vehicles (EV). As SOC is not measureable during vehicle operation, an onboard adaptive algorithm is developed in this paper. The algorithm estimates six electrical parameters for Li-ion batteries and provides a reliable SOC based on one of the estimated battery parameters, i.e. open circuit voltage (OCV). Simulation and vehicle validation results show good robustness and adaptation of the algorithm with high computational efficiency and low implementation cost.**

I. Introduction

Recently Li-ion batteries become promising as an energy storage component in plug-in hybrid electric vehicles (PHEV) and electric vehicles (EV). In order to better control the propulsion system in PHEV/EV, accurate knowledge of battery state of charge (SOC) is necessary. Battery SOC defines the remaining charge as a percentage of the stored charge in a fully charged battery [1-5]. However, battery SOC cannot be measured during vehicle operation. It can only be obtained through onboard estimation.

A battery parameter that is directly related to battery SOC is the open circuit voltage (OCV), which is the steady terminal voltage of a battery in open circuit. The OCV increases as battery SOC increases. The relationship between OCV and SOC can be acquired through experiments. The knowledge of other battery parameters is important to diagnostics and power management as well.

For some Li-ion batteries such as the iron phosphate Li-ion battery, a flat mapping curve from the OCV to battery SOC makes the SOC estimation even more difficult. Since the OCV is obscured by other dynamic voltage components under load, to get an accurate OCV estimate, the battery parameter estimation algorithm needs to subtract all the accountable voltage components from the terminal voltage. This requires a powerful algorithm to extract more battery parameters corresponding to more voltage components with high efficiency and accuracy. In consideration of the measurement error from in-vehicle sensors, it requires the algorithm be highly robust to initial conditions, environment variations, and measurement noise.

Manuscript received September 27, 2010.

Xidong Tang is with General Motors, Global R&D, 30500 Mound Road, Warren, MI 48090 USA (phone: 586-298-0254; fax: 586-986-3003; e-mail: xidong.tang@gm.com).

Xiaofeng Mao is with General Motors, Global R&D, 30500 Mound Road, Warren, MI 48090 USA (e-mail: xiaofeng.mao@gm.com).

Jian Lin is with General Motors, Global Vehicle Engineering, 30001 Van Dyke Road, Warren, MI 48090 USA (e-mail: jian.lin@gm.com).

Brian Koch is with General Motors, Global Vehicle Engineering, 30001 Van Dyke Road, Warren, MI 48090 USA (e-mail: brian.j.koch@gm.com).

There are a few methods in the literature on battery SOC estimation [1-7]. The most common method is based on Coulomb counting due to its simplicity for implementation. However, this method has two issues that largely limit its application to PHEV/EV. First, the Coulomb counting method has to start from a correct initial SOC, which is not always known. Second, the error will accumulate over time because of the presence of sensing errors. The magnitude of the error is dependent on sensor accuracy, current magnitude, and trip length. Moreover the Coulomb counting method requires the knowledge of battery capacity and does not have the ability to recover from a wrong SOC value. Another well known method is voltage based SOC correction as in [1]. In general an equilibrium voltage is measured after the battery rests for a long time (typically several hours), and is considered as the OCV. The OCV is then used to find the correct SOC through a lookup table. However, such a several-hour rest is very rare in the PHEV and EV applications. Recently, new methods estimating OCV online and inferring SOC from the estimated OCV have been developed in [2-3]. Similar methods that treat the OCV as an internal variable and estimate SOC directly from a battery model have also been developed in [4-5]. These methods open the door to the design of onboard battery SOC estimation algorithms. Other methods based on reduced electrochemical models are also introduced as in [6-7].

This paper proposes a practical approach to extract all six internal parameters adaptively from a second-order Li-ion battery model, which is identified and validated with lab collected data. Battery OCV, as one of the six parameters, is used to further infer battery SOC. Other parameters, such as the ohmic resistance and the time constants of diffusion and double layer, can be used for onboard diagnostics and power prediction (which will not be covered in this paper due to the space limit). The approach applies a well-known recursive least square (RLS) estimation technique [12-13] to the battery parameter estimation problem for two purposes.

The first purpose is to adaptively estimate more battery parameters in real time for SOC estimation and other potential applications with less predetermined look-up tables. Such a solution offers better adaptation to the environment and driving conditions. Meanwhile as an onboard application, the algorithm has to be designed for high computational efficiency as well as low implementation cost. The second purpose is to achieve high accuracy and robustness in battery parameter estimation, especially for the OCV. This is a necessary condition of providing an accurate and reliable SOC for battery control and electrical power management.

II. BATTERY MODEL IDENTIFICATION

Equivalent circuit models [2-3, 5, 8-11] can be used to represent the electrical property of Li-ion batteries. The OCV can be modeled as a high-valued capacitor or a voltage source. The remainder of the equivalent circuit includes a battery's ohmic resistance and one or several RC pairs, which characterize different battery dynamics such as the double layer effect and the diffusion effect. The order of the equivalent circuit model order should be determined by a tradeoff between the model complexity and precision.

A. Model Order

To determine the order of a battery model, we use the hybrid pulse power characterization (HPPC) test data. The HPPC profile that is designed to evaluate dynamic power capability consists of repetitions of a discharge pulse and a charge pulse at different temperatures, current rates, and SOC levels [15]. For each repetition, the HPPC test cycles batteries with a 10 second discharge pulse (with a current rate being 10C/5C/3C) followed by a same rate 10 second charge pulse. The test is conducted on different types of Li-ion. Fig. 1 shows the voltage response to a pair of 3C discharge and charge pulses at 5% SOC for a manganese-based Li-ion battery. Fig. 2 shows the voltage response to a pair of 5C discharge and charge pulses at 65% SOC for an iron phosphate Li-ion battery.

The discrete time model of Li-ion batteries can be represented by a difference equation, which can be written into a general form as:

$$V(k) = \theta^T \varphi(k) \tag{1}$$

where $V(k)$ is the measured battery terminal voltage, $\varphi(k)$ is a vector of measured data and known signals consisting of terminal voltage and current as well as known constants, θ is a vector of parameters to be estimated, and k indicates the time step. In particular, for a first order battery model, θ is a vector of four parameters as $\theta = [\theta_1, \theta_2, \theta_3, \theta_4]^T$, and the corresponding vector of signals and known constants is $\varphi(k) = [V(k-1), I(k), I(k-1), 1]^T$, where $I(k)$ is the measured battery terminal current. Similarly, for a second order battery model, θ becomes a vector of six parameters as $\theta = [\theta_1, \theta_2, \theta_3, \theta_4, \theta_5, \theta_6]^T$. The vector of signals and known constants becomes $\varphi(k) = [V(k-1), V(k-2), I(k), I(k-1, Ik-2, 1]T$.

Battery models with different orders have been established and simulated against the HPPC data. As shown in Fig. 1 and Fig. 2, a second-order linear model closely matches the battery dynamic behavior characterized by the HPPC test data, while a first-order model is proved not to able to capture the dynamic response of the voltage. The explicit expression of a second order battery model can be rewritten as

$$V(k) = \theta_1 V(k-1) + \theta_2 V(k-2) + \theta_3 I(k) + \theta_4 I(k-1) + \theta_5 I(k-2) + \theta_6. \tag{2}$$

It is verified that the second-order model fits the HPPC data very well for all test conditions. The model parameters vary with temperature, SOC and battery ages as well. However, compared with the time constants of battery dynamics, the parameters are slow time-varying and can be treated as local constants that change slowly with time. Therefore the dependence of the parameters on temperature, SOC, and battery degradation is handled via a forgetting factor.

B. Battery Parameter Identification

The parameters θ in (2) need to be associated with battery electrical parameters such as OCV and the ohmic resistance. After a parameter estimation algorithm estimates θ based on (2), the battery electrical parameters can be inferred from θ.

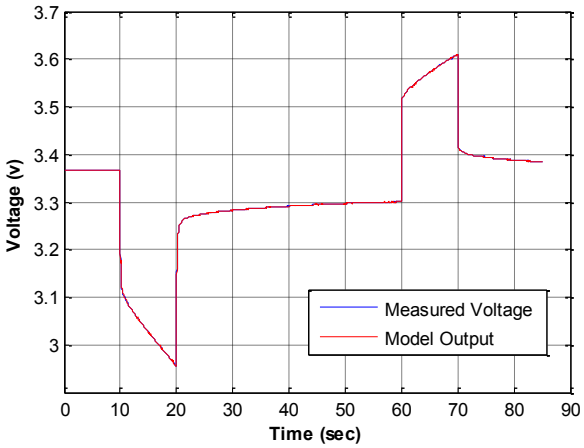

Fig. 1. Matching of model output and HPPC data for a manganese-based Li-ion battery at 20°C and 5% SOC.

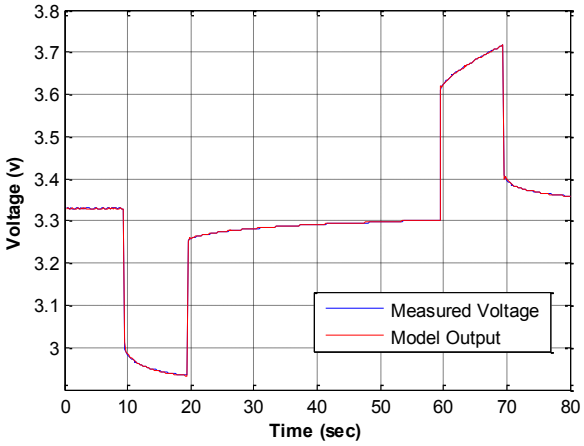

Fig. 2. Matching of model output and HPPC data for an iron phosphate Li-ion battery at 25°C and 65% SOC.

It is known that two main chemical processes determine the dynamic response of Li-ion batteries, that is, the diffusion and double layer. Consequently the battery terminal voltage consists of four parts, which can be expressed as

$$V(k) = V_{oc} + I(k)R_{ohm} + V_{dl}(k) + V_{df}(k) \tag{3}$$

where V_{oc} is the OCV, R_{ohm} is the ohmic resistance, and V_{dl} and V_{df} (voltages across the two RC pairs) are the double

layer voltage and the diffusion voltage, respectively. It is worth mentioning that each of two chemical processes is not necessarily to be characterized by one RC pair. In fact the chemical processes are more complicated than a linear representation and there are more than two chemical processes that affect the battery dynamic behavior.

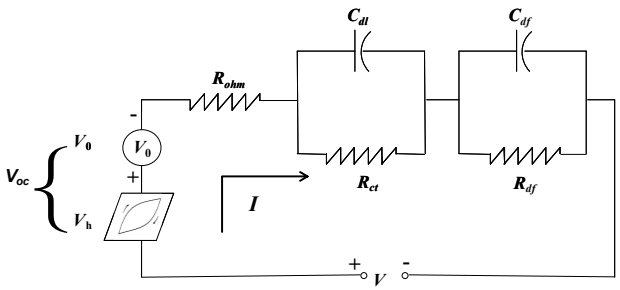

Fig. 3. The two-RC-pair battery circuit model for a Li-ion battery.

As shown in the previous section, the dynamic behavior of a Li-ion battery can be characterized as a second-order system approximately. In [4-5], equivalent circuits are used to model different types of batteries. This paper uses the same technique to model the Li-ion battery electrical property. To characterize a second-order system, a two-RC-pair equivalent circuit shown in Fig. 3 is widely used.

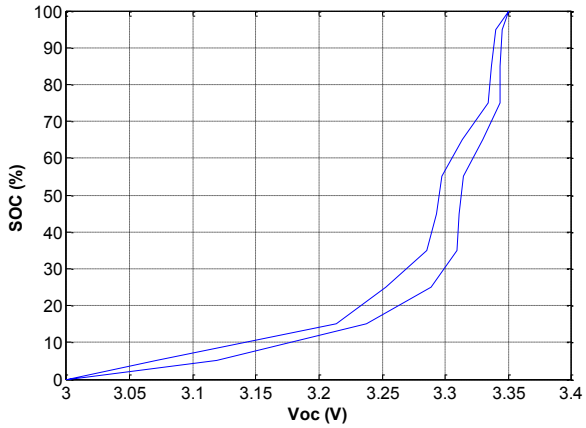

Fig. 4. Battery hysteresis of an iron phosphate Li-ion battery.

In Fig. 3, R_{ct} is the charge transfer resistance, C_{dl} is the double layer capacitance, R_{df} is the diffusion resistance, and C_{df} is the diffusion capacitance. The R_{ct}-C_{dl} pair is used to account for the dynamics of the double layer, and the R_{df}-C_{df} pair for the diffusion. For some batteries, the relationship between OCV and SOC is history and path dependent. This phenomenon is known as battery hysteresis, resulting in a nonlinear many-to-many mapping between OCV and SOC. It should be noted that battery hysteresis is a static phenomenon which distorts the one-to-one OCV-to-SOC static mapping. To compensate for the battery hysteresis, the OCV is further divided into two parts: V_o and V_h, where V_o is the thermodynamic voltage which has a one-to-one relationship to SOC, and V_h represents the battery hysteresis voltage. The sum of V_o and V_h gives V_{oc}. Different hysteresis models can be used to model different types of battery hysteresis such as in [3, 14]. The hysteresis effect in manganese-based Li-ion batteries is negligible, while iron phosphate Li-ion batteries exhibit an obvious hysteresis, as shown in Fig. 4. However, for iron phosphate Li-ion batteries, the hysteresis converges to its boundaries quickly enough to be modeled as a two-state switch. A simple switch type hysteresis model can be used to account for such a hysteresis effect (to be elaborated later).

With the zero-order hold (ZOH) discretization method, the dynamics of the double layer voltage V_{dl} and the diffusion voltage V_{df} in the discrete time form can be described by

$$\begin{aligned} V_{dl}(k) &= a_1 V_{dl}(k-1) + b_1 I(k-1) \\ V_{df}(k) &= a_2 V_{df}(k-1) + b_2 I(k-1) \end{aligned} \tag{4}$$

where

$$\begin{aligned} a_1 &= \exp(-\Delta t/(R_{ct}C_{dl})) \\ b_1 &= R_{ct}\left(1-\exp(-\Delta t/(R_{ct}C_{dl}))\right) \\ a_2 &= \exp\left(-\Delta t/(R_{df}C_{df})\right) \\ b_2 &= R_{df}\left(1-\exp\left(-\Delta t/(R_{df}C_{df})\right)\right) \end{aligned} \tag{5}$$

Based on (3) and (4), the two-RC-pair battery circuit model can be written into the state space form:

$$\begin{aligned} \begin{bmatrix} V_{dl}(k) \\ V_{df}(k) \end{bmatrix} &= A \begin{bmatrix} V_{dl}(k-1) \\ V_{df}(k-1) \end{bmatrix} + BI(k-1) \\ V(k) - V_{oc} &= C \begin{bmatrix} V_{dl}(k) \\ V_{df}(k) \end{bmatrix} + DI(k) \end{aligned} \tag{6}$$

where $A = \mathrm{diag}(a_1, a_2)$, $B = [b_1 \quad b_2]^T$, $C = [1 \quad 1]$, and $D = R_{ohm}$. The transfer function from the battery terminal current to the battery terminal voltage can be expressed as

$$\begin{aligned} V(z) - V_{oc} &= C(zI_{2\times 2} - A)^{-1}BI(z) + DI(z) \\ &= \left(\frac{b_1(z-a_2)+b_2(z-a_1)}{(z-a_1)(z-a_2)} + R\right) I(z) \end{aligned} \tag{7}$$

By taking the inverse z-transform, the discrete-time model can be organized into the following difference equation:

$$\begin{aligned} V(k) = {} & (a_1+a_2)V(k-1) - a_1a_2V(k-2) + R_{ohm}I(k) \\ & +[b_1 - b_2 - R_{ohm}(a_1+a_2)]I(k-1) \\ & +(a_1a_1R_{ohm} - b_1a_2 - b_2a_1)I(k-2) \\ & +[1-(a_1+a_2)+a_1a_2]V_{oc} \end{aligned} \tag{8}$$

where a_i and b_i, $i = 1,2$, are functions of the resistance and capacitance of the two RC-pairs. Comparing the two-RC-pair equivalent circuit model (8) and the second order battery model (2), one can establish the relationship between the battery electrical parameters and θ:

$$\begin{aligned} \theta_1 &= a_1 + a_2 \\ \theta_2 &= -a_1a_2 \\ \theta_3 &= R_{ohm} \\ \theta_4 &= b_1 - b_2 - R_{ohm}(a_1+a_2) \end{aligned}$$

$$\theta_5 = a_1 a_2 R_{ohm} - b_1 a_2 - b_2 a_1$$
$$\theta_6 = (1 - (a_1 + a_2) + a_1 a_2) V_{oc}. \quad (9)$$

The battery electrical parameters, i.e. V_{oc}, R_{ohm}, R_{ct}, C_{dl}, R_{df} and C_{df}, can be derived from (9) after acquiring θ. In particular, V_{oc} can be calculated by

$$V_{oc} = \theta_6/(1 - \theta_1 - \theta_2). \quad (10)$$

III. Adaptive Battery Parameter Estimation

For the Li-ion battery model described by the difference equation (1), we apply the U-D factorization-based RLS estimation method [12-13] to the battery parameter estimation problem. The difference between the classical RLS and the U-D factorization-based RLS is that the positive definite covariance matrix P is further factorized as $P = UDU^T$, where U is an upper triangular matrix and D is a diagonal matrix. The matrix P is not updated directly, instead, it is updated through multiplication of the updated values of U and D. The U-D factorization-based RLS method has been successfully used in many industrial applications due to its computational efficiency and stability. Assuring the positive-definiteness and symmetry of the covariance matrix, the method achieves high estimation accuracy and robustness.

The assumption of the estimation process is that the battery can be modeled as a linear time-invariant system under a certain operation condition. An adaptive algorithm is developed based on the above assumption. Given a sequence of current and voltage data: $I(k)$ and $V(k)$, the algorithm estimates the parameters in θ and then calculate the battery electrical parameters from θ. The adaptive six-parameter estimation algorithm consists of the following steps:

Step 1: The algorithm starts with initialization. Read the first two pairs of data $V(k)$ and $I(k)$, k=1,2. Set the initial values for θ as the estimate from previous operation stored in nonvolatile memory (NVM). Initialize the covariance matrix P by setting appropriate U and D. Define a forgetting factor λ satisfying $0 < \lambda \leq 1$.

Step 2: Read a new pair of data $V(k)$ and $I(k)$.

Step 3: Calculate $\varphi(k)$ from the present data $V(k)$ and $I(k)$, the data from the previous readings, $V(k\text{-}1)$, $V(k\text{-}2)$, $I(k\text{-}1)$ and $I(k\text{-}2)$.

Step 4: Let $\alpha_0 = \lambda$. Define two vectors f and g as

$$f = [f_1, \ldots, f_n]^T = U^T(k-1)\varphi(k)$$
$$g = [g_1, \ldots, g_n]^T = D(k-1)f \quad (11)$$

Step 5: For $j = 1,2, \ldots,6$, go through Step 5.1-5.2.

Step 5.1: Compute the following:

$$\alpha_j = \alpha_{j-1} + f_j g_j$$
$$D(k)_{jj} = (\alpha_{j-1} D(k-1)_{jj})/(\alpha_j \lambda)$$
$$b_j = g_j$$
$$c_j = -f_j/\alpha_{j-1} \quad (12)$$

Step 5.2: For $i = 1,2, \ldots, j-1$, go to Step 5.2.1 (if $j = 1$, skip Step 5.2.1).

Step 5.2.1: Compute the followings:

$$U(k)_{ij} = U(k-1)_{ij} + b_i c_j$$
$$b_i = b_i + U(k-1)_{ij} b_j \quad (13)$$

Step 6: Compute

$$L(k) = [b_1, \ldots, b_n]^T/\alpha_n \quad (14)$$

Step 7: Compute the estimation error as

$$\beta(k) = V(k) - \theta^T(k-1)\varphi(k) \quad (15)$$

Step 8: Update θ to minimize the estimation error β by

$$\theta(k) = \theta(k-1) + L(k)\beta(k) \quad (16)$$

Step 9: Calculate the battery electrical parameters V_{oc}, R_{ohm}, R_{ct}, C_{dl}, R_{df} and C_{df} from θ based on (9).

Step 10: Determine whether it is the end of operation. If yes, save θ to NVM for next operation and end the algorithm. Otherwise, save the current data $V(k)$ and $I(k)$ for next update and go back to Step 2 and continue the update.

IV. SOC Estimation

When the battery electrical parameters are obtained from the battery parameter estimation algorithm, in particular, the OCV, a voltage-based SOC_V can be inferred.

In the presence of battery hysteresis, the relationship between OCV and SOC is not a one-to-one mappinp. Such a nonlinear relationship can be generalized as follows:

$$SOC_V = h(V_{oc}, V_h). \quad (17)$$

As discussed in Section II, a switch type of hysteresis model can be used to model the battery hysteresis for iron phosphate Li-ion batteries. The model defines an additional hysteresis voltage V_h in OCV. By taking out the hysteresis voltage from OCV, the remaining voltage V_o can be monotonically mapped to SOC. The remaining V_o, called the thermodynamic voltage, is defined as the difference between V_{oc} and V_h:

$$V_o(k) = V_{oc}(k) - V_h(k). \quad (18)$$

For the switch type of hysteresis model, V_h is governed by

$$V_h(k) = V_h(k-1) + \theta_7 I(k-1)[V_{hmax} - \text{sign}(I(k-1)V_h(k-1))] \quad (19)$$

where θ_7 is a parameter to determine convergence rate, and V_{hmax} defines the boundaries of battery hysteresis. The

values of θ_7 and V_{hmax} can be obtained through experiments and vary with OCV (i.e. SOC). The hysteresis model in (19) describes a type of hysteresis with fast convergence to hysteresis boundaries from any point inside the boundary loop. With such a switch type of hysteresis model, the voltage -based SOC_V is robust to the initial hysteresis voltage, that is, it is not necessary to require accurate knowledge of the initial hysteresis voltage because the hysteresis voltage governed by the model quickly converges to boundaries wherever it starts.

The SOC estimation algorithm combines the voltage-based SOC_V and a current-based SOC_I through Coulomb counting. The final SOC estimate is a weighted combination of SOC_V and SOC_I as

$$\mathrm{SOC}(k) = w\mathrm{SOC_I}(k) + (1-w)\mathrm{SOC_V}(k) \qquad (20)$$

where $0< w <1$ is the weighting factor. The combined SOC(k) will be used as a new starting point for the next update at the time instant k +1. The benefit is to reduce the dependency on the initial SOC and increase algorithm robustness.

The weighting factor w is tuned based on the signal excitation level. For instance, the value of w decreases by 5% when the excitation level is lower than a threshold at the present time instant k. On the other hand, the value of (1- w) decreases by 5%, when the excitation level is higher than another threshold at the present time instant k. The signal excitation level can be evaluated through monitoring the six elements in the diagonal matrix D or the determinant of D. It should be noted that real Li-ion batteries are not an ideal linear time invariant system. The model given by (2) is a simplified one for the estimation purpose, matching the Li-ion battery dynamics under a specific operation condition. Model uncertainties as well as the shifting of operation conditions, in combination with the use of the forgetting factor λ, will cause the increase of the values in one or several of the six elements in D, which should be decreasing in an ideal case of linear time invariant systems.

Following the battery parameter estimation algorithm in Section III, the SOC estimation algorithm is as follows:

Step 1: Starting with initialization, the algorithm sets the initial value of SOC(0) by reading the estimation result of previous operation from ROM.

Step 2: Obtain V_{oc} from the battery parameter estimation algorithm and determine the validity of the estimated V_{oc}. If V_{oc} is not valid, set the weighting factor w =0 and go to Step 7.

Step 3: Update V_h using (18).

Step 4: Calculate V_o using (17).

Step 5: Infer $\mathrm{SOC_V}(k)$ from V_o at the present time step.

Step 6: Tune the weighting factor w for SOC_V and SOC_I based on the signal excitation level.

Step 7: Read data $I(k)$ and calculate the $\mathrm{SOC_I}(k)$ via

$$\mathrm{SOC_I}(k) = \mathrm{SOC_I}(k-1) + I(k)\Delta t \qquad (21)$$

where $\mathrm{SOC_I}(k-1)$ is from the previous time step, and $I(k)\Delta t$ is the contribution from the Coulomb counting.

Step 8: Calculate the combined SOC(k) using (20)

Step 9: Determine whether it is the end of operation. If yes, save SOC(k) to NVM for next operation and end the algorithm. Otherwise, go back to Step 2 and continue the estimation.

V. Results

The developed algorithm is evaluated through laboratory collected data and vehicle data. The evaluation results of manganese-based Li-ion batteries are shown in Fig. 5 and Fig. 6. Fig. 5 shows the trajectories of an offline calculated SOC and the SOC estimate from the algorithm for a charge depletion drive. The calculated SOC is manually derived from the OCV measured before and after the drive, and the measured current during the drive. The battery rests for hours in order to measure OCV. The measured OCV is used to find the reference SOC. The calculated SOC is compared with the SOC estimate. It can be seen from Fig. 5 that the overall estimation error is within 3% in this case.

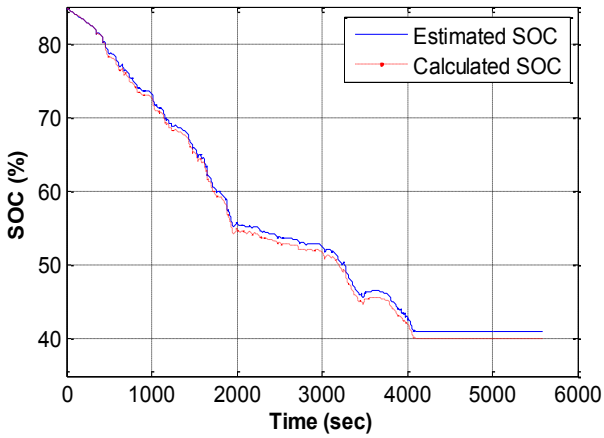

Fig. 5. Algorithm evaluation on a charge depletion drive for a 30AH manganese-based Li-ion battery pack.

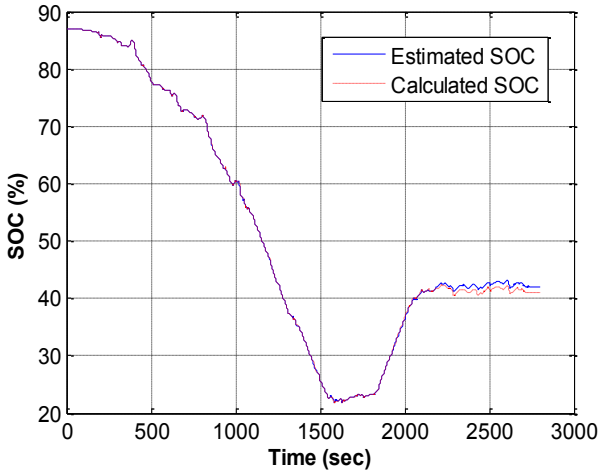

Fig. 6. Algorithm evaluation on a charge depletion-charge sustaining-charge increase drive for a 45AH manganese-based Li-ion battery pack.

Fig. 6 shows the trajectories of a calculated SOC and the SOC estimate from the algorithm for a charge depletion-charge sustaining-charge increase drive. Note that the battery capacity is different from the case shown in Fig. 5. As shown in Fig. 6, the overall estimation error is within 3% as well.

Fig. 7 shows the evaluation result for an iron phosphate Li-ion battery pack, containing trajectories of the three SOC estimates from the algorithm and the calculated SOC for reference. From Fig. 7, it can be seen that SOC_I is unable to recover from a wrong initial point, while SOC_V is robust to initial values. It is also noted that after SOC_V is blended with SOC_I, the combined SOC shows improved stability.

To evaluate algorithm robustness to sensor noise, a white noise of amplitude 20mV, an even distribution noise of amplitude 5mV, and a sinusoidal noise of amplitude 5mV are added to the measured terminal voltage. Moreover, a white noise of amplitude 1.8A, an even distribution noise of amplitude 0.25A, and a sinusoidal noise of amplitude 0.25A are added to the measured terminal current. Consider that for iron phosphate Li-ion batteries, SOC changes 10% for about 20mV change in OCV. Hence the injected noise is significant. However, it can be seen from Fig. 8 that the injected noise has no significant impact on the SOC estimate. Both trajectories converge to the actual SOC (measured and back calculated offline) within acceptable errors.

VI. Conclusion

In the paper, an adaptive battery parameter estimation algorithm is developed for onboard SOC estimation. The developed algorithm has been verified through simulation and in-vehicle testing. The results show effectiveness in SOC estimation and robustness to initial conditions, battery variations, and operation environment. The battery parameters estimated by the developed algorithm can also be used for other applications such as onboard diagnostics and power prediction.

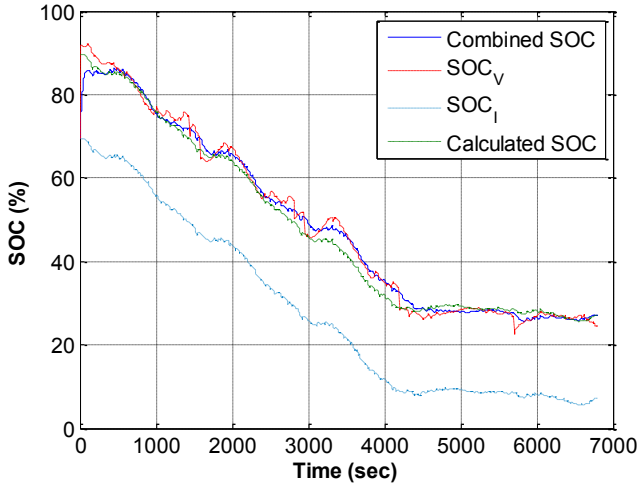

Fig. 7. Algorithm evaluation on a charge depletion-charge sustaining drive for an iron phosphate Li-ion battery pack.

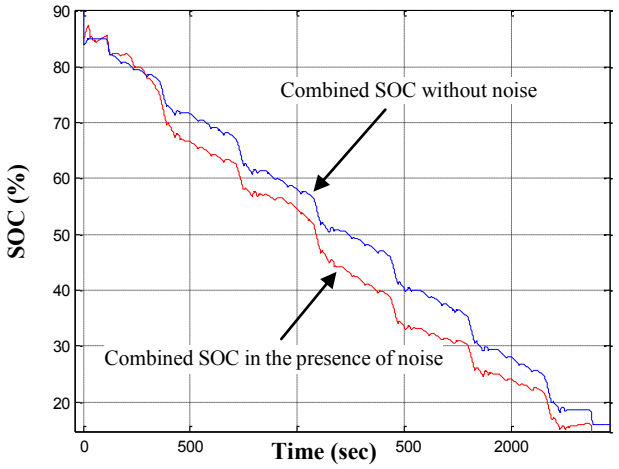

Fig. 8. Algorithm evaluation in the presence of voltage and current noise.

References

[1] Z. He, M. Gao, and J. Xu, "EKF-Ah based state of charge online estimation for lithium-ion power battery," in *2009 International Conference on Computational Intelligence and Security*, vol. 1, pp.142-145.

[2] M. Verbrugge, D. Frisch, and B. Koch, "Adaptive energy management of electric and hybrid electric vehicles," *Journal of The Electrochemical Society*, vol. 152, no. 2, pp. A333-A342, 2005.

[3] M. Verbrugge and E. Tate, "Adaptive state of charge algorithm for nickel metal hydride batteries including hysteresis phenomena," *Journal of Power Sources*, vol. 126, pp. 236-249, 2004.

[4] H. Dai, Z. Sun, and X. Wei, "Online SOC estimation of high-power lithium-ion batteries used on HEVs," in *2006 IEEE International Conference on Vehicular Electronics and Safety*, pp. 342-347.

[5] G. L. Plett, "Extended kalman filtering for battery management systems of LiPB-based HEV battery packs," *Journal of Power Sources*, vol. 134, pp. 252–292, 2004.

[6] R. Klein, Chaturvedi, N.A., J. Christensen, J. Ahmed, J., Findeisen and A. Kojic, "State estimation of a reduced electrochemical model of a lithium-ion battery," *in Proceedings of the 2010 American Control Conference*, pp. 6618-6623, 2010.

[7] N. Chaturvedi, R. Klein, J. Christensen, J. Ahmed, and A. Kojic, "Algorithms for advanced battery-management systems," *IEEE Control Systems Magazine*, vol. 30, no. 3, pp. 49-68, 2010.

[8] S. Bhatikar, R. Mahajan, K. Kipke, and V. Johnson, "Neural network based battery modeling for hybrid electric vehicles," in *Proceedings of the 2000 Future Car Congress*, Paper No. 2000-01-1564, Arlington, VA.

[9] H. Chan and D. Sutanto, "A new battery model for use with battery energy strorage systems and electric vehicle power systems," in *proceedings of the 2000 IEEE Power Engineering Society Winter Meeting*, Singappre, 23-27.

[10] V. Johnson, A. Pesaran, and T. Sack, "Temperature-dependent battery models for high-power lithium-ion batteries," in *Proceedings of the 17th Electric Vehicle Symposium*, Montreal, Canada, 15-18 Oct. 2000.

[11] S. J. Lee, J. H. Kim, J. M. Lee, and B. H. Cho, "The state and parameter estimation of an Li-ion battery using a new OCV-SOC concept," in *2007 IEEE Power Electronics Specialists Conference*.

[12] G. J. Bierman, *Factorization Methods for Discrete Sequential Estimation*. New York: Academic, 1977.

[13] L. Ljung and T. Soderstrom, *Theory and Practice of Recursive Identification*. Cambridge, MA: MIT Press, 1983.

[14] X. Tang, X. Zhang, B. Koch, and D. Frisch, "Modeling and estimation of Nickel Metal hydride battery hysteresis for SOC estimation," in *Proceedings of the 2008 Internationa Conference on Prognostics and Health Management*, Denver, Colorado.

[15] PNGV batery test manual, INEEL, DOE/ID-10597, Review 3, 2001.